Volume 17, Number 5, 2024. pp. 621-627

Jordan Journal of Physics

ARTICLE

Effect of Reaction Time on Structure, Morphology and Optical Energy Gap of TiO_2 Nanorods Prepared by One-Step Hydrothermal Method

Hersh Ahmed Khizir and **Tariq Abdul-Hameed Abbas**

Department of Physics, College of Science, Salahaddin University, Erbil 44001, Iraq.

Doi: **https://doi.org/10.47011/17.5.9**

Received on: 07/06/2023; *Accepted on: 20/09/2023*

Abstract: In this study, well-aligned rutile TiO_2 nanorod arrays were grown on fluorine-doped tin oxide (FTO) substrates by a hydrothermal technique using $TiCl_4$ as the titania precursor. The influence of hydrothermal reaction (growth) time on the change of nanostructure shape and size during the preparation of the nanorods was examined. The study investigated the characteristics of the prepared TiO_2 nanorods using various analytical techniques, such as X-ray diffraction (XRD), field emission scanning electron microscopy (FESEM), Raman spectroscopy, and UV-visible spectrophotometer. Diverse structures, morphologies, and optical band gaps of TiO_2 nanorods were obtained by varying the hydrothermal reaction time at optimized growth factors such as growth temperature, precursor concentration, and acidity. The composition remained rutile, although the particle size and the average diameter of the nanorods changed with the growth time. It was observed that the absorption edge shifted to longer wavelengths (redshift), and the predicted band gap of TiO2 decreased as the growth time increased. Additionally, the rutile phase was confirmed through Raman spectroscopic analysis.

Keywords: TiO_2, FTO, One-step Hydrothermal, Growth time, Nanorods.

1. Introduction

Recently, metal oxides have become increasingly important in the fields of nanoelectronics and materials science [1]. Metal compounds are employed in both conductive and dielectric applications [2]. Microelectronic circuits, sensors, piezoelectric devices, and fuel cells are just a few of the applications for metal oxides [2]. High conductors, superconductors, semiconductors, and insulators are the four types of metal oxides. All metal-based nanocomposites have specific applications and share common properties [3]. Among the various types of metal oxides, titanium dioxide (TiO_2) has attracted much interest due to its properties, making it suitable for various technological applications [4]. This interest can be attributed to its photoinduced reactivity and distinctive electrical characteristics. Titanium dioxide (TiO_2, rutile, Eg = 3.05 eV) nanostructures are considered promising materials for use in all types of photovoltaic systems [5]. Single-crystal nanorods or nanowires provide direct electrical pathways for photogenerated electrons, which can potentially improve the electron transport rate in photovoltaic systems such as dye-sensitized solar cells (DSSCs) [6]. The crystalline structure, particle size, optical properties, and morphology of TiO_2 are crucial factors for these applications. Therefore, one of the most important aspects of advancing TiO_2 nanoscience is the ability to control the size and morphology of the material for specific applications [7].

Corresponding Author: Hersh Ahmed Khizir **Email**: hersh.khizir@su.edu.krd

TiO_2 exists in three polymorphs (phases): rutile, anatase, and brookite. Both rutile and anatase have a tetragonal crystalline structure, while brookite has an orthorhombic structure [8][9]. Rutile and anatase are the most commonly used polymorphs of TiO_2, with rutile being more stable at room temperature than anatase and brookite. Numerous one-dimensional TiO_2 nanostructures, including nanowires [11], nanotubes [12], and nanobelts [13], have been fabricated using various methods, such as hydro-solvothermal methods [14, 15], sol-gel template processes [16], thermal oxidation [17], chemical vapor deposition [18], and microwave-assisted hydrothermal methods [19]. Among these, the hydrothermal approach is considered the optimal method for fabricating TiO_2 nanorods, as it offers several advantages, including the production of high-quality materials with small diameters, low cost, and ease of use [5].

In this study, oriented TiO_2 nanorods were synthesized on FTO substrates using a one-step hydrothermal technique by varying the reaction time. This approach aimed to produce high-quality TiO_2 nanorods with good crystallite orientation due to the growth processes. The resulting nanorods were subsequently analyzed for their structural, optical, and surface morphological properties. Different sizes and diameters of TiO_2 nanorods were obtained by varying the hydrothermal growth time, which also influenced the crystallinity, morphological features, and band gap energy.

2. Experimental Section

2.1 TiO_2 Nanorods Arrays Preparation

The one-step hydrothermal method was used to grow TiO_2 nanorod arrays on FTO-coated glass (8 Ω/sq) of 2.2 mm thickness. First, the FTO-coated glass was cut into 2.5 × 2.5 cm pieces to be used as substrates. The substrates were cleaned with acetone, deionized water, and ethanol in an ultrasonic bath. After that, by using a Teflon-lined stainless-steel autoclave, 30 mL of deionized water was mixed with 30 mL of strong hydrochloric acid (37% by weight) and 0.65 mL of titanium tetrachloride ($TiCl_4$) to get a total volume of 60 mL in a typical synthesis 100 mL in volume. The mixture was agitated rapidly for 25 minutes using a magnetic stirrer to achieve a translucent and clear solution. After stirring the mixed solution, the cleaned substrate was fixed against the Teflon-liner wall with the conducting side facing upward. This setup allowed for the growth of a thin layer of TiO_2 on the substrate once it had been cleaned. The volume ratio of $HCl:H_2O:TiCl_4$ was 30:30:0.65 mL, and samples were prepared for various growth times (2, 6, and 12 hours) at an optimized hydrothermal reaction temperature of 170 °C, as reported in our previous work [20]. After the growth process, the autoclave was allowed to cool, and the samples were cleaned with deionized water and dried in an oven at 70 °C for 1 hour.

2.2 Characterizations

The morphology of the samples was studied using field emission scanning electron microscopy (FESEM). The structural properties and elemental composition of the TiO2 nanorods were investigated using X-Ray diffraction (XRD) with a PAN analytical X'Pert PRO (Cu Kα = 1.5406 A°). Optical measurements were performed using a Shimadzu UV-Vis Mini 1240 spectrophotometer in the wavelength range of 200–1100 nm. Raman spectra were recorded in the wavenumber range of 200–1800 cm^{-1} using a Jobin-Yvon Horiba LABRAM-HR Raman spectrometer.

3. Results and Discussion

3.1 XRD Study

Figure 1 displays the XRD patterns of prepared TiO_2 nanorods at different reaction times (2, 6, and 12 h). The figure depicts that all the peaks of the samples are indexed to the rutile phase of TiO_2 and well matched to the standard JCPDS file no: 77–0452 for tetragonal rutile TiO_2 polymorphs [20]. All of the patterns exhibit the same diffraction peaks at positions 2θ values of the prepared samples at reaction time of 12 h: (27.3221°), (36.0044°), (39.1223°), (41.1640°), (43.9033°), (54.2467°), (56.5357°), (62.7009°), (63.9482°), and (68.8361°) corresponding to crystal planes of the rutile phase (110), (101), (200), (111), (210), (211), (220), (002), (130), and (301), respectively. With protraction, the extremely strong intensity of the (110) peak suggests that the nanorods are well-crystallized and oriented perpendicular to the substrate along the (110) direction.

Further, from the broadening of the diffraction peak and by using Scherrer's

equation, the average crystallite size (D) has been estimated [21]:

$$D = \frac{0.9\,\lambda}{\beta\cos(\theta)} \quad (1)$$

where λ is the X-ray wavelength, β is the full width at half maximum of the peak (in radians), and θ is Bragg's angle (in degrees). The determined crystallite size of TiO_2 nanoparticles hydrothermally produced at varied reaction times of 2, 6, and 12 h was found to be 17.03, 59.30, and 41.54 nm, respectively (Table 1).

This suggests that the reaction time plays a crucial role in the growth of the nanorods. Well-crystallized TiO_2 nanorods are formed when the growth time is 12 h. The Ti_3O_5 phase disappears with increasing reaction time as Ti and O atoms combine to form TiO_2. Therefore, the formation of TiO2 nanorods is facilitated by increasing the reaction time.

The competition between dissolution and crystal growth could lead to the peeling off of the nanorods [22]. At shorter growth times, the supersaturation of the precursor is high, promoting the growth of the nanorods. In contrast, for longer growth times, the crystal growth rate decreases as the system approaches equilibrium. In this case, crystal dissolution may become significant on high-energy surfaces, such as the surface of TiO_2 nanorods. This interface is strained and may dissolve, even though the rest of the nanorods are in equilibrium with the solution due to the lattice mismatch between the FTO and rutile nanorods.

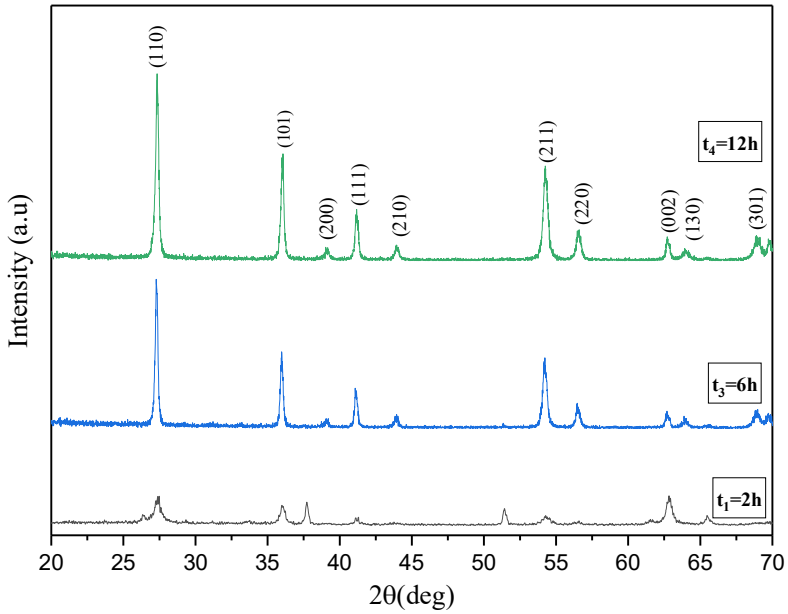

FIG. 1. XRD patterns of TiO_2 nanorods prepared at different hydrothermal reaction times (2, 6, and 12 h).

TABLE 1. Measured structural and morphological parameters of TiO_2 nanorods synthesized at different hydrothermal reaction times (2, 6, and 12 h).

Growth time (h)	Energy gap (eV)	2θ (deg)	β (FWHM) (deg)	Crystallite size D (nm)	Average diameter (nm)
2	3.078	27.3538	0.4800	17.03	64.26
6	3.023	27.1629	0.1378	59.30	143.28
12	2.989	27.3221	0.1968	41.54	186.13

3.2 Morphological study

Figure 2 shows micrographs of TiO_2 nanorods synthesized at three reaction times (2, 6, and 12 h). As the growth time increases from 2 to 12 hours, the diameter of the nanorods grows from 64.26 to 186.13 nm. With the continued increase in reaction time, the neighboring nanorods begin to agglomerate. This phenomenon is attributed to the increased number of TiO_2 nuclei, which affects the radial growth of the nanorods. This result is consistent with the XRD findings. As the growth time increases, the length of the nanorods remains essentially unchanged, while the quadrate side

length decreases. The structure and morphology parameters of the prepared samples are summarized in Table 1. The rutile phase is clearly observed for all growth times, as indicated by the measured structural and morphological parameters of the TiO_2 nanorods.

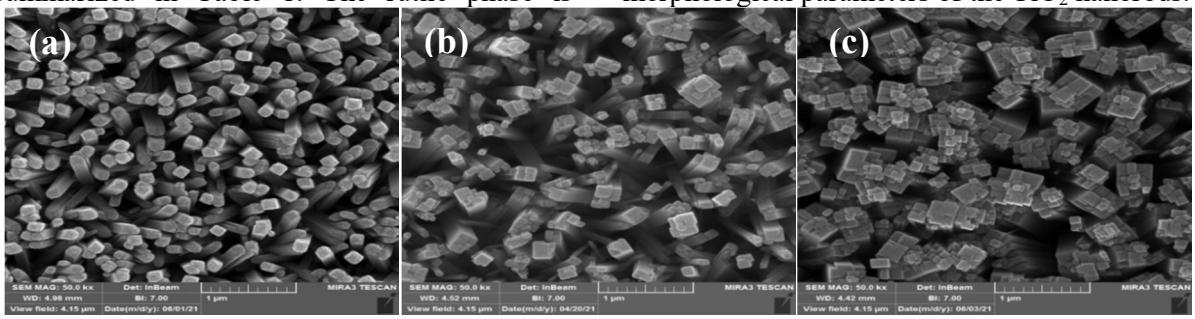

FIG. 2. FESEM images of TiO_2 nanorods prepared at different hydrothermal reaction times: (a) 2 h, (b) 6 h, and (c) 12 h.

3.3 Optical Study

The TiO_2 nanorods were analyzed for their optical properties in terms of energy band gaps. The energy band gaps of these nanorods for a direct transition were obtained from the UV–visible spectroscopy by taking into account the Fahrenbruch and Bube relation described by Eq. (2) [23].

$$\alpha h\vartheta = A(h\vartheta - E_g)^{\frac{1}{2}} \quad (2)$$

where α is the absorption coefficient, hν is the photon energy, A is a constant, and E_g is the energy gap. Figure 3 illustrates how the linear portion of $(\alpha h\nu)^2$ against photon energy (hν) plots can be used to get the direct optical band gap values. The band gaps of the synthesized TiO_2 at different reaction times (2, 6, and 12 h) were determined to be 3.078, 3.023, and 2. 989 eV, respectively. It is clear that the energy band gap decreases as the growth time increases, which can be attributed to changes in the TiO_2 nanorod sizes as a function of growth time. This trend is consistent with the XRD and FESEM analyses. The structural, morphological, and optical parameters of the prepared samples are summarized in Table 1.

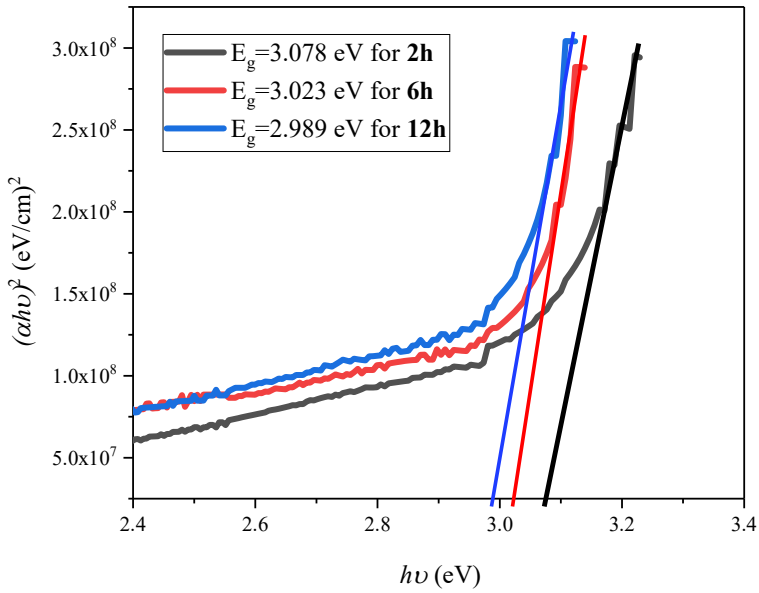

FIG. 3. The $(\alpha h\nu)^2$ versus hν plots of TiO_2 nanorods prepared at different hydrothermal reaction times (2, 6 and 12 h).

3.3.1 Raman Analysis

The crystalline nature of TiO_2 nanorods was further characterized by Raman spectroscopic analysis. The typical Raman spectrum of the aligned TiO_2 nanorods synthesized with a growth time of 6 h is displayed in Fig. 4. The measurement was carried out in the range of 200-900 cm^{-1}. The Raman scattering reveals the presence of rutile Raman-active modes. The rutile structure belongs to the P42/mnm tetragonal space group having three Raman active modes: E_g, A_{1g}, and second-order

scattering [24]. These characteristic bands are observed at wavenumbers of 237.722, 443.85, and 603.03 cm^{-1} from the TiO_2 nanorods, as illustrated in Fig. 4. The spectrum exhibits intense peaks at 443.85 and 603.03 cm^{-1}, which correspond to the Raman-active modes E_g and A_{1g} of rutile TiO_2, respectively. The spectrum also exhibits a broad peak at 237.722 cm^{-1}, which may be due to the second-order scattering. The Raman analysis results confirmed the highly crystalline rutile structure of the synthesized TiO_2 nanorods. The appearance of the Raman modes has also been confirmed by XRD and FESEM analyses.

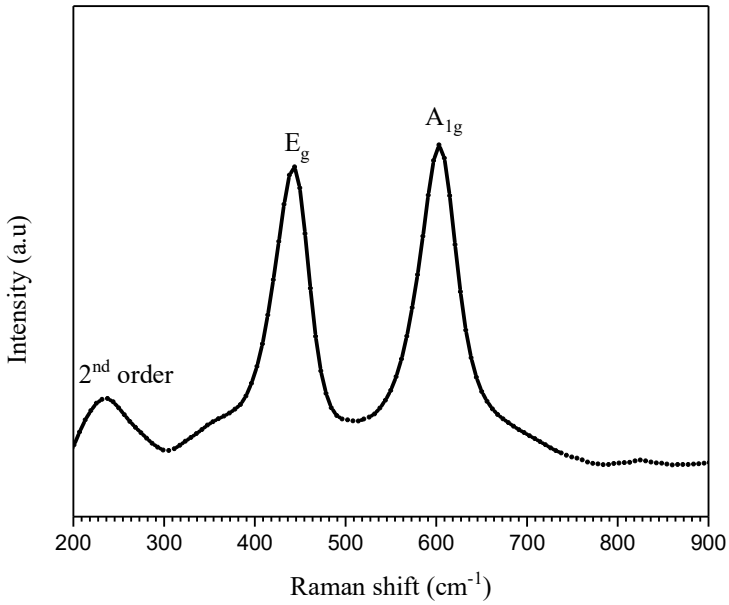

FIG. 4. Raman spectrum of the TiO_2 nanorods synthesized with a hydrothermal growth time of 6 h.

Finally, it is necessary to mention the objective of this study, which is one of the most noteworthy aspects of the present work. The objective of this work was to synthesize nanorods using a one-step hydrothermal technique, investigating the influence of hydrothermal growth time on the shapes and sizes of the nanostructures. Table 2 provides a comparison of the structural and morphological parameters of the synthesized TiO_2 nanorods from this study with previously published data. The overall results confirm that the hydrothermal reaction time has a significant impact on the shape and size of the nanostructures during the hydrothermal process. Interestingly, as a potential future application, it can be concluded that controlling the shape and size of the nanostructures is a crucial parameter for the fabrication of light-emitting diodes and dye-sensitized solar cell layers.

TABLE 2. The measured structural and morphological parameters of the synthesized TiO_2 nanorods in this study, compared with other reported results.

Source of Titanium	Solvents (acid or base)	Reaction Time (h)	Band gap energy	Phase of the TiO_2	Morphology, dimensions, etc.	Ref.
Titanium tricloride	distilled water	0.5 - 2	----------	Rutile	Nanorods D=20nm, L=250 nm	[25]
Titanium tetra iso-propoxide (TTIP)	NaOH (10 M) aqueous solution	10 and 16	3.6 eV and 3.5 eV	Anatase	Nanotubes	[26]
$TiCl_4$	HCl aqueous solution	3, 4.5 and 7.5	---------	Rutile	Nanorods D=165, 175, 190 and 210	[4]
Titanium butoxide	HCl aqueous solution	1, 2, 3, and 4	3.35—3.1	Rutile	Nanorods D=50-150nm	[27]
Titanium tetraisopropoxide	Ethanol, and glacial acetic acid	1, 2, and 3	2.91, 2.96, and 2.98	Anatase	Nanorods D=14.6-10.9nm	[28]
$TiCl_4$	HCl aqueous solution	2--12	3.078—2. 989	Rutile	Nanorods D=64.26-186.13nm	Pressent work

4. Conclusion

TiO_2 nanorods were prepared successfully using the hydrothermal technique. The influence of hydrothermal growth time on the change of nanostructures' shapes and sizes during the preparation of the nanorods was studied. It was shown that the properties of the prepared TiO_2 nanorods can be controlled by the hydrothermal growth time. Structural characterization confirms the sharp and well-defined peak formation of TiO_2 nanorods related to the rutile phase, with the relative intensities of the peaks varying with the reaction time. Well-crystallized TiO_2 nanorods were formed when the reaction time was 6 or 12h. Morphological analysis showed that the evolution of formed TiO_2 nanorods can be modified by controlling the reaction time. When the growth time increased from 2 to 12 h, the diameter of the nanorods increased from 64.26 to 186.13 nm. Optical measurements indicated that the energy band gap decreased from 3.078 to 2.989 eV with increasing reaction time. Additionally, Raman spectroscopy confirmed the presence of the rutile phase of TiO_2. In conclusion, the control of reaction time significantly influences the properties of TiO_2 nanorods, providing valuable insights for the development of optimal layers for applications in polymer solar cells and light-emitting diodes.

Conflict of Interest: There are no conflicts of interest declared by the authors.

References

[1] Naseem, T. and Durrani, T., Environ. Chem. Ecotoxicol., 3 (2021) 59.

[2] Fernández-garcia, M. and Rodriguez, J.A., Brookhaven National Lab.(BNL), (2007) (No. BNL-79479-2007-BC).

[3] Omprakash, S.S., Kumar, N., and Holla, S., Mater Today Proc., 5 (2018)10833.

[4] Iraj, M., Nayeri, F., Asl-soleimani, E., and Narimani, K., J. Alloys Compd., 659 (2015) 44.

[5] Guo, F. et al. J. Mater. Sci. Mater. Electron., 29 (2018) 12169.

[6] Rho, W., Jeon, H., Kim, H., Chung, W., Suh, J., and Jun, B., J. Nanomater., 16 (2015) 85.

[7] Bade, B., Rondiya, S., Bhopale, S., Dzade, N., and Kamble, M., SN Appl. Sci., 1 (2019) 1.

[8] Wicaksana, D., Kobayashi, A., Kinbara, A., Wicaksana, D., Kobayashi, A., and Kinbara, A., J. Vac. Sci. Tecnol. A., 10 (1992) 1479.

[9] Wilson, G., Matijasevich, A., Mitchell, D., Schulz, J., and Will, G., Langmuir., 22 (2016) 2016.

[10] Lv, M. et al., Nanoscale, 4 (2012) 5872.

[11] Qader, A. and Faisal, D., J. Mater. Sci. Mater. Electron., 26 (2015) 317.

[12] Ge, M. et al., Adv. Sci., 4 (2016) 1600152.

[13] Lu-Lu, L. and Jin-Ming, W., J. Mater. Chem. A, 3 (2015) 15868.

[14] Sorapong, P., Supachai, N., Yoshikazu, S., and Susumu, Y., Mater. Res. Soc. Symp. Proc., 951 (2007) 2.

[15] Kathirvel, S., Su, C., Shiao, Y., Lin, Y., Chen, B., and Li, W., Sol. Energy, 132 (2016) 310.

[16] Attar, A., Mirdamadi, S., Hajiesmaeilbaigi, F., and Ghamsari, M., J. Mater. Sci. Technol., 23 (2007) 611.

[17] Lee, G. and Lee, G., Mater. Res. Innov., 8917 (2016) 1.

[18] Jie, W., Guo, R., Jeffrey, A., Guangwen, Z., and Vijay, K., Res. Soc. Symp. Proc., 879 (2005) 712.

[19] Jia, X., He, W., Zhang, X., and Zhao, H., Nanotechnology, 18 (2007) 075602.

[20] Khizir, H. and Abbas, T., J. Sol-Gel. Sci. Technol., 98 (2021) 487.

[21] Mahshid, S., Askari, M., and Ghamsari, M., J. Mater. Process Technol., 189 (2007) 296.

[22] Liu, B., Enache-Pommer, E., and Aydil, E., J. Am. Chem. Soc., 131 (2010) 3985.

[23] Yesappa, L. et al., J. Electron. Mater., 46 (2017) 6965.

[24] Huo, K. et al., J. Nanosci. Nanotechnol., 9 (2009) 3341.

[25] Guobin, M., Xiaoning, Z., and Jianmin, Z., Int. J. Mod. Phys. B, 19 (2005) 2763.

[26] Ranjitha, A., Muthukumarasamy, N., Thambidurai, M., Velauthapillai, D., Agilan, S., and Balasundaraprabhu, R., Int. J. Light Electron. Opt. 126 (2015) 17.

[27] Hashim, S., Salman, O., and Hassoon, K., Int. J. Eng. Technol., 39 (2021) 1133.

[28] Ulhaq, M. and Kusumawardani, C., Indones. J. Chem., 5 (2022) 17.